Front. Earth Sci. 2015, 9(3): 427–436
DOI 10.1007/s11707-014-0458-3

RESEARCH ARTICLE

Interpretations of gravity and magnetic anomalies in the Songliao Basin with Wavelet Multi-scale Decomposition

Changbo LI[1,2], Liangshu WANG (✉)[1], Bin SUN[1], Runhai FENG[1], Yongjing WU[1]

1 School of Earth Sciences and Engineering, Nanjing University, Nanjing 210046, China
2 Nanjing Institute of Geology and Mineral Resources, Nanjing 210016, China

Abstract In this paper, we introduce the method of Wavelet Multi-scale Decomposition (WMD) combined with Power Spectrum Analysis (PSA) for the separation of regional gravity and magnetic anomalies. The Songliao Basin is situated between the Siberian Plate and the North China Plate, and its main structural trend of gravity and magnetic anomaly fields is NNE. The study area shows a significant feature of deep collage-type construction. According to the feature of gravity field, the region was divided into five sub-regions. The gravity and magnetic fields of the Songliao Basin were separated using WMD with a 4th order separation. The apparent depth of anomalies in each order was determined by Logarithmic PSA. Then, the shallow high-frequency anomalies were removed and the 2nd–4th order wavelet detail anomalies were used to study the basin's major faults. Twenty-six faults within the basement were recognized. The 4th order wavelet approximate anomalies were used for the inversion of the Moho discontinuity and the Curie isothermal surface.

Keywords gravity and magnetic anomalies, Songliao Basin, deep structure and geodynamics, Wavelet Multi-scale Decomposition, Power Spectrum Analysis

1 Introduction

Gravity and magnetic methods are commonly used in basin structural interpretation because of their better horizontal resolution, compared to seismic profile exploration (Liu et al., 1996). However, observed gravity and magnetic anomalies are the superposition of anomalies induced by geologic bodies at different depths (Xu et al., 2009). The separation of regional residual anomalies is one of the important tasks in gravity and magnetic interpretation. A lot of anomaly separation methods have been developed based on different characteristics of regional and residual fields, such as polynomial surface fitting (Beltrão et al., 1991), the minimum curvature method (Mickus et al., 1991), the 3D magnetic inversion algorithm (Li and Oldenburg et al., 1998), and finite element analysis (Mallick and Sharma, 1999). Recently, wavelet transformation has been widely used in the processing and interpretation of gravity and magnetic anomalies because of its good ability to do multi-scale analysis. Traditional spectrum analysis is usually used to assist wavelet analysis with finding the depth of gravity and magnetic anomalies (Albora et al., 2001). In this study, we used wavelet transformation combined with spectrum analysis to separate gravity and magnetic anomalies in the Songliao Basin and to examine the basin's deep structures and geodynamics.

The longitude and latitude of the investigated area ranges from 118°E to 132°E and from 40°N to 52°N (Fig. 1), including the Songliao Basin and its adjacent area. The Songliao Basin is one of the typical basins among the NE China Basin Groups including the Songliao Basin, the Hailar Basin, and the Sanjiang Basin. These basins are located in the north of the circum-pacific tectonic belt, situated between the Siberian Plate and the North China Plate (Fig. 1). There are lots of fold belts around the Songliao Basin, such as the Daxing'anling Mountains hercynian fold belt in the west, the Xiaoxing'anling Mountains fold belt in the north, the Qinglong-Hulan Caledonian fold belt in the south, and the Zhangguangcai Mountains hercynian fold belt in the east (Ren et al., 2002). The basement of the Songliao Basin mainly consists of metamorphic sandstone, griotte, slate, and large-scale hercynian and Caledonian intrusive granite (Wu et al., 2001). Many authors have studied the deep structures and geodynamics of the Songliao Basin using geophysical

Received September 6, 2013; accepted March 13, 2014

E-mail: lswang@nju.edu.cn

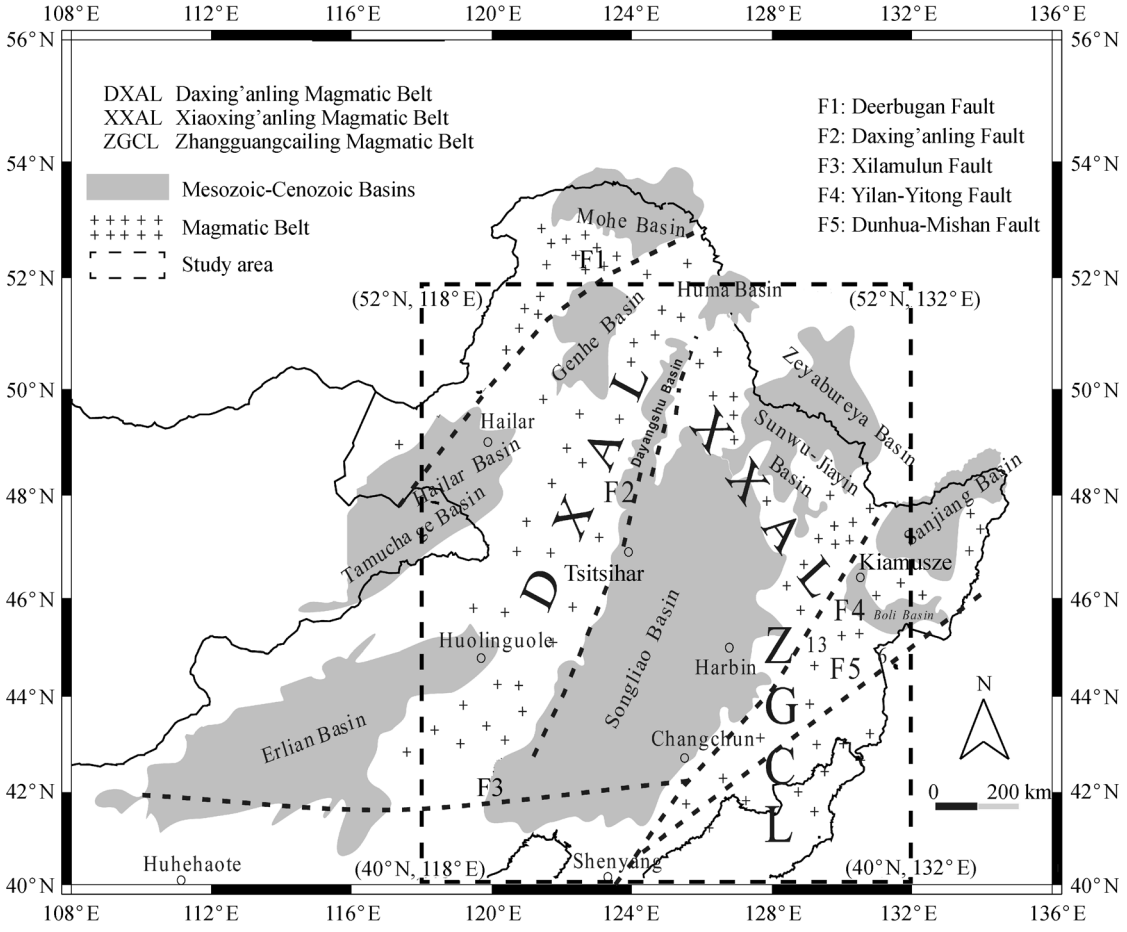

Fig. 1 The location of study area (Revised from Sun et al., 2012)

methods (e. g., Duncan and Richards, 1991; Zhang et al., 1995; Bi, 1997; Ai et al., 2003; Li and Yuan, 2003; Zhao et al., 1994; Huang and Zhao, 2006; Li, 2006; Li et al., 2008; Shen and Zhou, 2009; Zhang et al., 2010; Zhu et al., 2010). These researchers have reached basic agreements about the geological background of the Songliao Basin. Most results show that the basin is closely related to the magma upwelling and lithospheric thinning caused by deep subduction of the Pacific Plate. Zhao (2004) has studied the effect caused by the pacific subduction zone by means of the seismic tomography of NE China. However, the study of the basement is insufficient to understand the fracture distribution. Furthermore, accurate maps of crustal interfaces, Moho discontinuity, and Curie isothermal surfaces are still not drawn, which also restricts the further understanding of the Songliao Basin's geodynamics.

2 Method and results

2.1 Theory of wavelet analysis

According to Wavelet Analysis Theory (Lee and Yamamoto, 1994), if $f(t) \in L^2(R)$, we define its wavelet transformation as:

$$W_f(a,b) = <f,\psi_{a,b}> = |a|^{-1/2}\int_{-\infty}^{+\infty} f(t)\overline{\psi\left(\frac{t-b}{a}\right)}\mathrm{d}t, \quad (1)$$

in which the Wavelet Function is

$$\psi_{a,b}(t) = |a|^{-1/2}\psi\left(\frac{t-b}{a}\right)(a \in R,\ a \neq 0;\ b \in R). \quad (2)$$

For $C_\psi = \int_{-\infty}^{+\infty}\frac{\left|\hat{\psi}(\omega)\right|^2}{|\omega|}\mathrm{d}\omega < \infty$, $\hat{\psi}(\omega)$ is the flourier transformation of $\psi(t)$, and we get the reverse wavelet transformation:

$$f(t) = C_\psi^{-1}\int_{-\infty}^{+\infty}\int_{-\infty}^{+\infty}(CWT_\psi f)(a,b)\psi_{a,b}(t)\frac{\mathrm{d}a}{a^2}\mathrm{d}b. \quad (3)$$

Make $a = a_0^j$, $b = ka_0^j b_0$, $a_0 > 1$, and $b_0 > 0$, then the wavelet transformation changes into the discrete version:

$$W_f(j,k) = a_0^{-\frac{j}{2}}\int_{-\infty}^{+\infty} f(x)\overline{\psi(a_0^{-j}x - kb_0)}\mathrm{d}x, \quad (4)$$

where $\psi_{jk} = a_0^{-\frac{j}{2}}\psi(a_0^{-j}x - kb_0)(j,k \in Z)$; make $a_0 = 2$, $b_0 = 1$, we get

$$\Psi_{j,k}(t) = 2^{-j/2\psi}(2^{-j}t - k), \tag{5}$$

and $W_f(j,k) = 2^{-\frac{j}{2}}\int_{-\infty}^{+\infty} f(x)\overline{\psi(2^{-j}x-k)}\mathrm{d}x.$ (6)

It can be proved that $\int_{-\infty}^{+\infty}\psi_{jk}(x)\overline{\psi_{mn}(x)}\mathrm{d}x = \delta_{jm,nk} = \begin{cases}1, j=m, k=n\\ 0, \text{else}\end{cases}$ consists of a set of standard independent bases belonging to $L^2(R)$. Accordingly, we get the wavelet transformation function:

$$f(x) = \sum_{j,k\in Z} W_f(j,k)\psi_{jk}(x). \tag{7}$$

Analogously, if the 2D gravity anomaly field is $\Delta G(x,y) = f(x,y)$, we use the Mallat (1989) method, according to Yang et al. (2001)'s deduction, the gravity's 4th decomposition expression can be written as

$$\Delta G = D_1G + D_2G + D_3G + D_4G + A_4G, \tag{8}$$

where $D_1G - D_4G$ belong to $W_1 - W_4$ and represent wavelet anomaly details from the 1st to 4th orders, and A_4G is the 4th order wavelet anomaly approximation.

2.2 Gravity and magnetic characteristics

The Bouguer gravity anomaly of the investigated area ranges from −119 mGal to 31 mGal (Fig. 2), and most of the gravity anomalies and gradient belts align in NE-NNE direction. This indicates that the existing EW-trending Paleo-Asian Ocean structure has been overlain with and altered by the late NE-trending Marginal Pacific structure (Sun et al., 2012), and it has been demonstrated that the transformation of the Paleo-Asian tectonic system into the circum-Pacific system took place during the Triassic period (Xu et al., 2009; Xiao et al., 2003). The Songliao Basin is a relatively high-valued gravity anomaly area, surrounded by a low amplitude anomaly. The anomaly's shape and orientation change frequently, but the change of gradient is very small. In the west there is a continuous significant gravity gradient belt, named Daxing'anling Mountains. It is about 100 km wide and ranges from −90 mGal to −30 mGal. The Hailar Basin, in the north of study area, also has a relatively high-valued gravity anomaly belt. In the east of the Songliao Basin, the character of the gravity anomaly turns NS-trending.

The study area shows a significant feature of deep collage-type construction consisting of several micro-plates. Based on the feature of gravity field, we divided the region into five sub-regions (Fig. 2). They are the Hailar-Erlian sub-region (I), the Daxing'anling Mountains gravity gradient belt sub-region (II), the Songliao Basin sub-region (III), the Xiaoxing'anling Mountains sub-region (IV), and the Zhangguangcai Mountains sub-region (V). These sub-regions agree well with the research conducted by Cheng (2006).

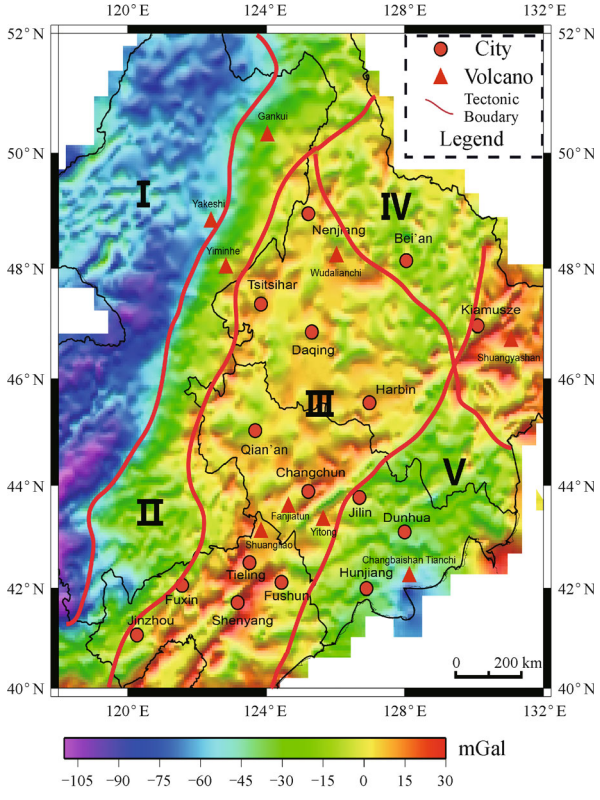

Fig. 2 Bouguer gravity anomaly of the Songliao Basin

In Fig. 3, the maximum magnetic anomaly is 1,324 nT and the minimum value is −609 nT. The trend of the magnetic anomaly is in the NE-NNE direction, consistent with the Bouguer anomaly map. The Songliao basin is a relatively low-negative magnetic anomaly area surrounded by a low-positive anomaly. The anomaly's shape is placid and its orientation changes smoothly because of the thick sedimentation. In the northwest, the magnetic anomaly is messy and turbulent because of the exposed magnetic granites.

2.3 WMD and PSA of gravity and magnetic anomalies

We used Wavelet Multi-scale Decomposition with 4th order separation to separate the gravity and magnetic anomalies in the study area based on the geological background and the estimation of the interfaces' depths. The decomposition results are shown in Figs. 4(a–j), and the corresponding spectrum results are in Fig. 5. From the spectrum results, we can estimate the average depths of the wavelet decomposition results at each order. We can see that the depths of D_1G (Fig. 4(a)) and D_1M (Fig. 4(f)) are 3.0 km and 2.6 km, respectively. They indicate that the 1st order of wavelet details of the gravity and magnetic anomalies can reflect signals from superficial bodies with high density and magnetism. $D_2G–D_4G$ (Fig. 4(b–d)) and $D_2M–D_4M$ (Fig. 4(g–i)) show the 2nd to 4th orders of wavelet details of the gravity and magnetic anomalies, their estimated depth is 9.6 km, 14.4 km, 25.7 km, 8.5 km, 13.2 km, and 21.5 km, respectively. They can reflect the character of the basement and middle crust. A_4G (Fig. 4(e)) and A_4M (Fig. 4(j)) show the 4th order wavelet anomaly approximation of the gravity and magnetic anomalies. The estimated depths of the 4th order wavelet approximation of the gravity and magnetic anomalies are 38.9 km and 26.7 km. They can reveal the ups and downs of deep interfaces such as the Moho discontinuity and the Curie isothermal surface.

3 Discussion

3.1 Basement faults

According to the results of WMD and PSA, we used the details of the 2nd and 3rd orders of the anomalies to study the basement structure of the Songliao Basin. In order to distinguish the basement faults, we calculated the horizontal derivations of the 2nd and 3rd orders of wavelet details of the gravity anomaly ($D_2G–D_3G$) in NW-SE ($DD_2–DD_3$), EW ($HD_2–HD_3$), and SN ($VD_2–VD_3$) directions (Fig. 6). According to the linear characteristics, we deduced 26 basement faults (Table 1).

Most of these faults are striking in the NE-NNE direction, consistent with the featured direction of the gravity anomaly and related to the effects of Pacific

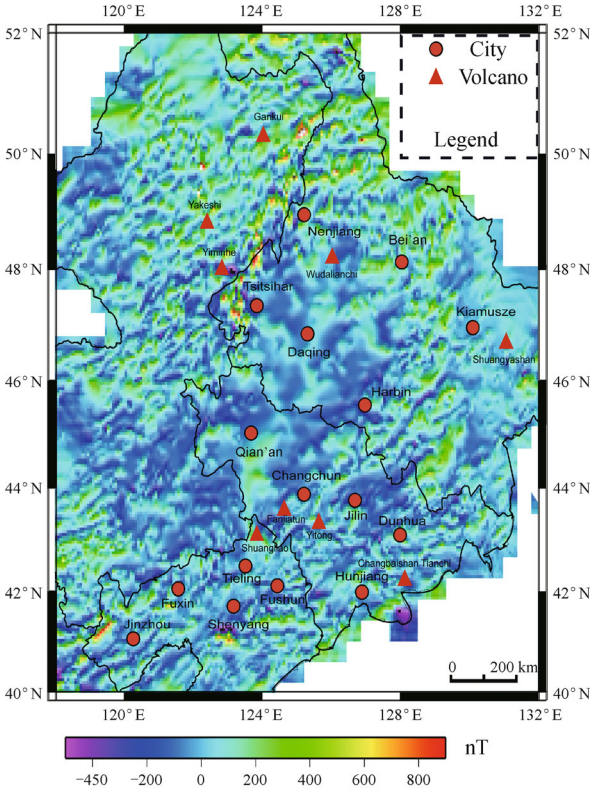

Fig. 3 Magnetic anomaly of the Songliao Basin

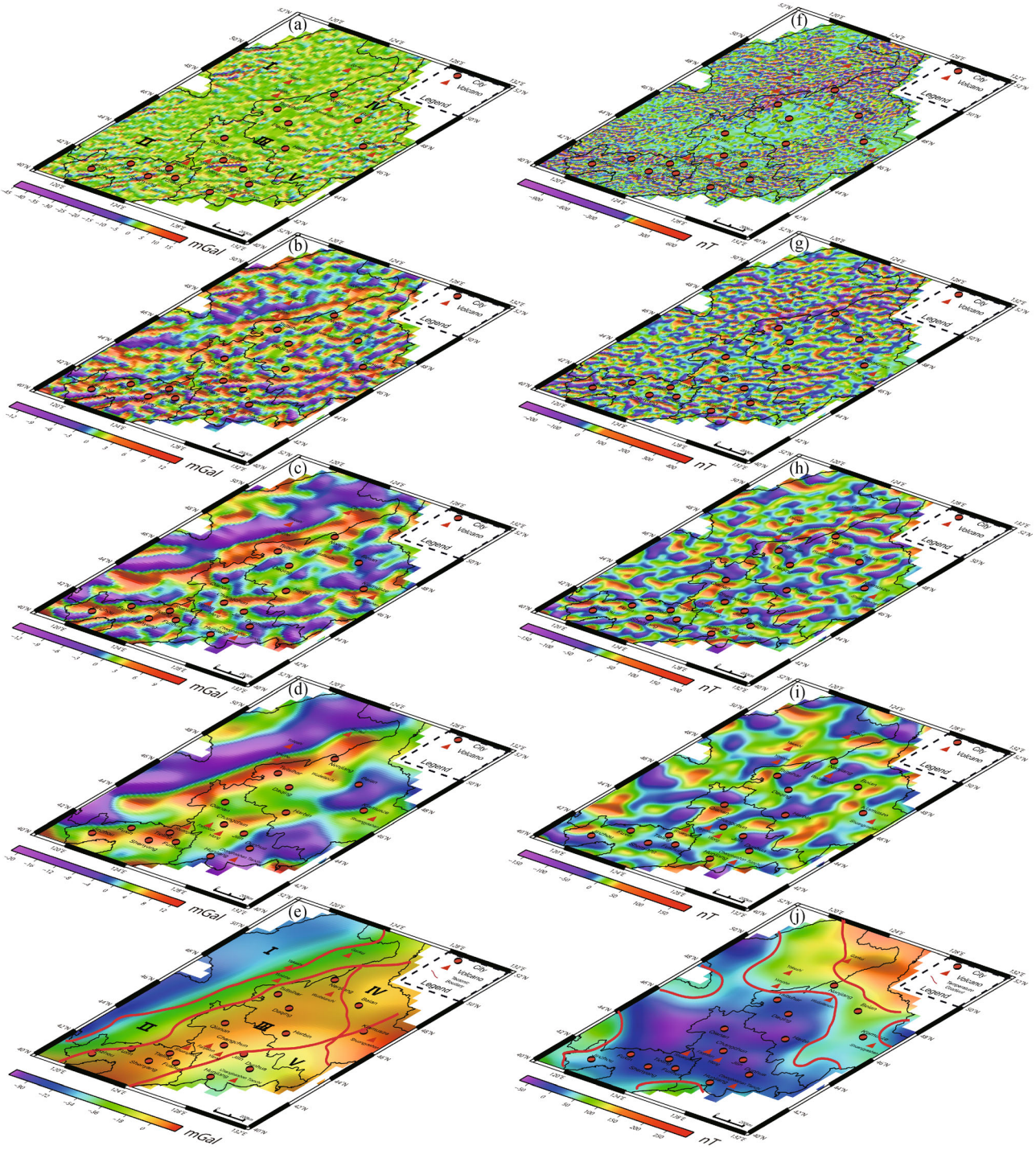

Fig. 4 WMD of gravity and magnetic anomalies in the Songliao Basin. (a–d) indicate the 1st to 4th orders of wavelet details of the gravity anomaly (D_1G–D_4G). (e) shows the 4th order wavelet approximation of the gravity anomaly (A_4G). (f–i) shows the 1st to 4th orders of wavelet details of the magnetic anomaly (D_1M–D_4M). (j) shows the 4th order wavelet approximation of magnetic anomaly (A_4M).

subduction. From DD_3, HD_3, and VD_3, we can pick out some of the deep faults, such as the F2, F4, F7, and F8. They may have cut through the shallow crust and reached the depth of 14.4 km at least. This situation is also suitable

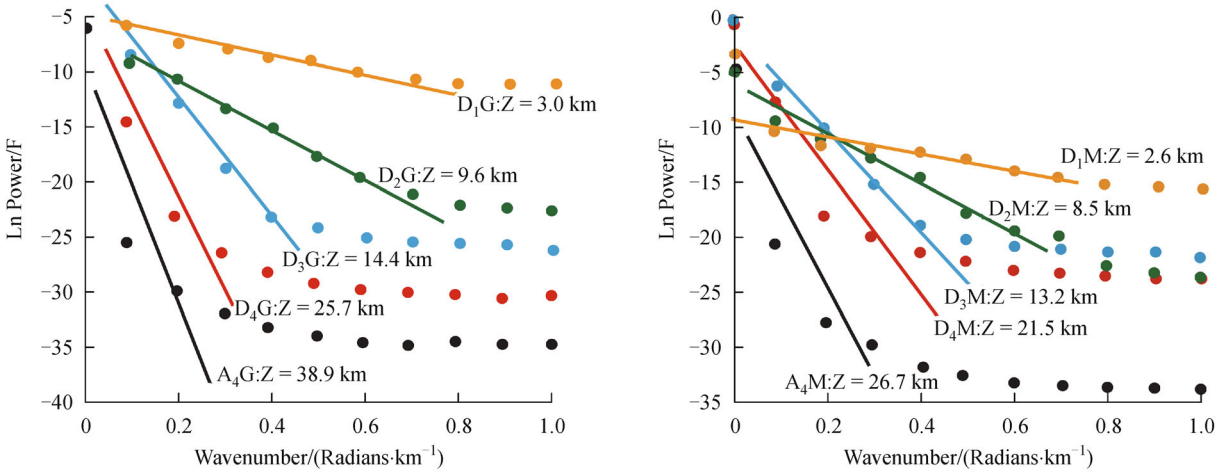

Fig. 5 PSA of gravity and magnetic anomalies in the Songliao Basin

for F10, F12 in HD_3, F17, F18, F19, and F25 in VD_3. However, additional geochemical evidence is needed to prove whether they are deep faults or not. Compared with Fig. 2, we can find that F2 exactly matches with the micro-plate boundary between the Hailar-Erlian sub-region (I) and the Daxing'anling Mountains gravity gradient belt sub-region (II). F7 is also located at the joint of the Songliao Basin sub-region (III) and the Zhangguangcai Mountains sub-region (V). This proves that the recognition of deep faults plays an important part in the determination of plate boundaries.

3.2 Moho discontinuity and Curie isothermal surface

The Moho discontinuity is the crust-mantle boundary, it is important to know its depth for the understanding of the geodynamics and deep tectonics of a given area. According to the seismic data of NE China, the assumed density difference between bottom crust and upper mantle is 0.43 g/cm^3. The average depth of Moho is 40 km (Yang et al., 1996). We used the 4th order wavelet approximation of the gravity anomaly to inverse the depth of the Moho discontinuity (Fig. 7).

The result shows that the depth of the Moho discontinuity in the study area is about 35 km on the average and ranges from 29.75 km to 40.75 km. From NW to SE, the Moho interface becomes deeper and deeper, which indicates that the regional structural trend is nearly NE. In the details, the Songliao Basin sub-region (III) is right in the uplifting center. Around this elliptic area, there are low and even mantle slopes. Combined with the characters of the 5 sub-regions (Fig. 2), we can easily find that the Daxing'anling Mountains mantle slope is consistent with the Daxing'anling Mountains gravity gradient belt sub-region (II). The Zhangguangcai Mountains mantle depression has the same slope as the Zhangguangcai Mountains subregion (V). Furthermore, we find that the major deep faults (e.g., F19, F3, F7) listed in Table 1 are all by the edge of the gradient belt of the Moho surface. This is due to the fact that the crust thickness always changes with the major faults (Sun et al., 2012).

The Curie isothermal surface is the depth at which temperature is about 580°C and the magnetic minerals lose their magnetism. For the Songliao Basin, the average depth of the Curie isothermal surface is 25 km and the assumed magnetization intensity difference at the interface is 2 A/m (Hu et al., 2006). We used the 4th order wavelet approximation of the magnetic anomaly to inverse the depth of the Curie isothermal surface (Fig. 8).

The result shows that the depth of Curie isothermal surface in the study area is about 25.5 km on the average and ranges from 16.5 km to 34.5 km. The Curie isothermal surface is generally uplifted in the center area, and depressed in the surrounding area. The volcanoes in the study area are located along the edge of the uplift of the Curie isothermal surface. The Songliao Basin is located almost in the most uplifted area, but in the interior of the basin the Curie isothermal surface has ups and downs, which indicates the heterogeneity of crustal structures and heat flow in the Songliao Basin. These features reveal the fact that the Songliao Basin is a complex extensional basin, but its geothermal gradient is affected by many factors.

4 Conclusions

For this study, we used the method of Wavelet Multi-scale

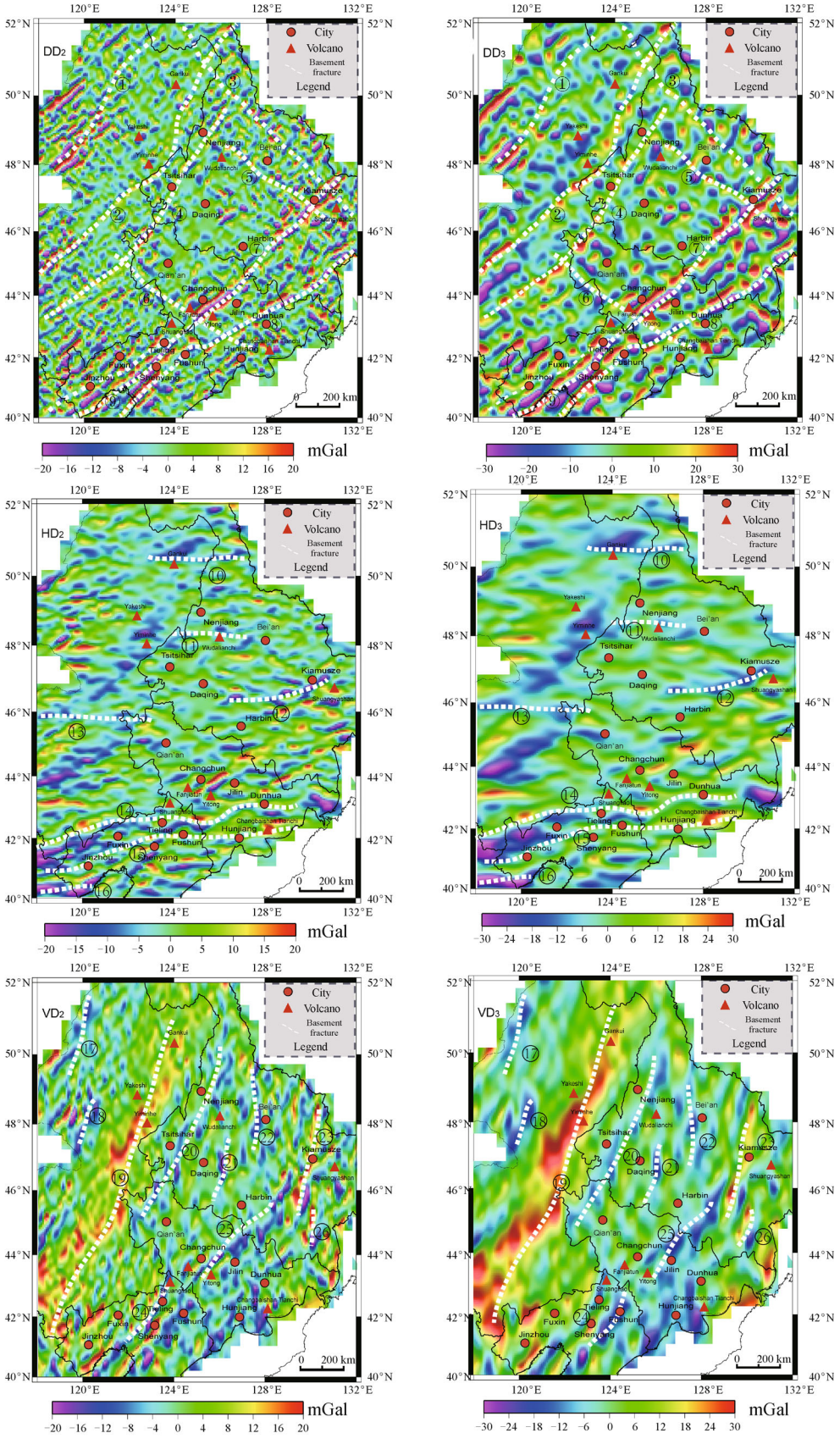

Fig. 6 The horizontal derivations of the 2nd and 3rd orders of wavelet gravity anomaly details in the NW-SE(DD_2–DD_3), EW(HD_2–HD_3), and SN(VD_2–VD_3) directions and estimated basement faults

Table 1 Estimated basement faults

No.	Fault name	Strike	Remarks
F1	Deerbugan	NE	Obviously observed in the 2nd and 3rd orders of wavelet gravity anomaly details horizontal derivation for the NW-SE direction. Among them, F2, F7, F9 can also be seen in the wavelet gravity anomaly details horizontal derivation for the SN direction.
F2, 19	Daxing'anling Mountains	NNE	
F3	Jiagedaqi-Hulin	NW	
F4	Erlian-Heihe	NE-NEE	
F5	Suihua-Mulan	NW	
F6	Fuyu-Dehui	NW	
F7, 25	Yilan-Yitong	NE	
F8	Dunhua-Mishan	NE	
F9, 24	Shanhaiguan-Fuxin	NE	
F10	Xiao Yangqi-Baishilazi	EW	Obviously observed in the 2nd and 3rd orders of wavelet gravity anomaly details horizontal derivation for the EW direction.
F11	Lane Moore River	EW	
F12	Huanan-Baoqing	EW	
F13	Samai-Hulitu	EW	
F14	Wenduermiao-Xilamulun	EW	
F15	Jining-Lingyuan	EW	
F16	Huailai-Xinglong	EW	
F17	Hula lake-Jilalin	NE	Obviously observed in the 2nd and 3rd orders of wavelet gravity anomaly details horizontal derivation for the SN direction. F19, F24, and F25 are the supplements of F2, F9, and F7.
F18	Tayuan-Xigui	NE	
F2, 19	Daxing'anling Mountains	NNE	
F20	Nenjiang-Baicheng	NE	
F21, 22	Bei'an-Daqing	NNE	
F23	Nancha	SN	
F9, 24	Shanhaiguan-Fuxin	NE	
F7, 25	Yilan-Yitong	NE	
F26	Mudangjiang	SN	

Decomposition to separate regional gravity and magnetic anomalies in the Songliao Basin and its adjacent area. Combined with previous geological and geophysical research results, we studied the deep structures of the Songliao Basin including basement faults, the depth of the Moho discontinuity, and the depth of the Curie isothermal surface, and then we discussed the basin's geodynamic and tectonic evolution.

The gravity and magnetic anomalies in the study area showed a significant feature of deep collage-type construction. The anomalies almost align in the NE-NNE direction, and the anomalies in the EW, and SN directions are mostly blurred and small-scale, which indicates that the NE-trending Pacific subduction is the latest tectonic event affecting the Songliao Basin's structure. According to the derivations of the 2nd and 3rd orders' wavelet gravity anomaly details in the NW-SE, EW, and SN directions, we have a systematic understanding of the study area's microplate boundaries and have estimated 26 potential basement faults. A_4G and A_4M are the 4th order wavelet approximations of the gravity and magnetic anomalies. With the inversion results of A_4G and A_4M, we generated the map of the Moho discontinuity and the Curie isothermal surface, We zoned the study area into the Songliao mantle uplifting center, the Daxing'anling Mountains mantle slope, the Zhangguangcai Mountains mantle depression, and the Songliao high geothermal gradient. They are all consistent with the features of gravity and magnetic anomalies.

On the basis of basement faults, volcanoes, and the map of the Moho discontinuity and the Curie isothermal surface, we agree with the conclusions of Zhao et al (1994), and Wang and Liu (1997), and argue that the Songliao Basin is a complex extensional basin, whose geodynamics are mainly affected by the Pacific subduction and some other factors like the heterogeneity of crustal structures. Because of the subduction of the Pacific plate, hot asthenosphere materials well up in the form of plumes, stimulating the occurrence of extensional rifts and faults that develop in the Songliao Basin.

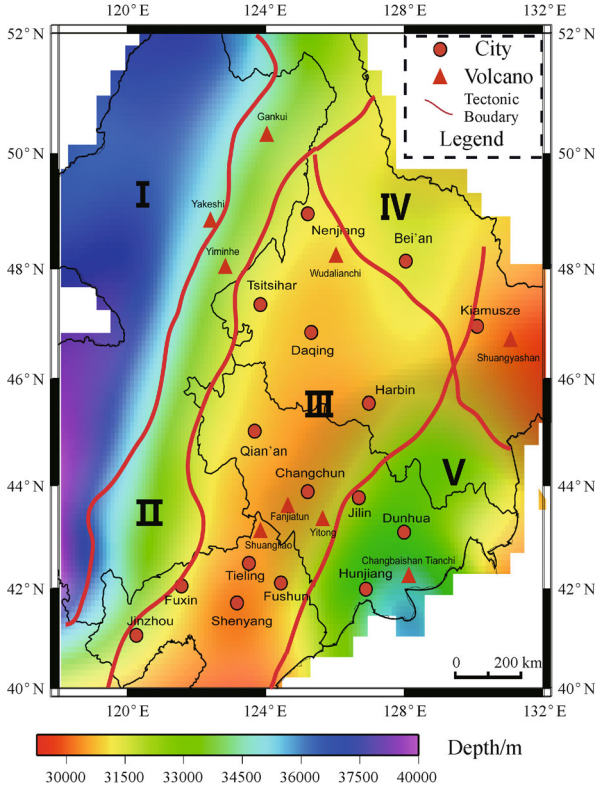

Fig. 7 Map of the depth of Moho surface in Songliao Basin

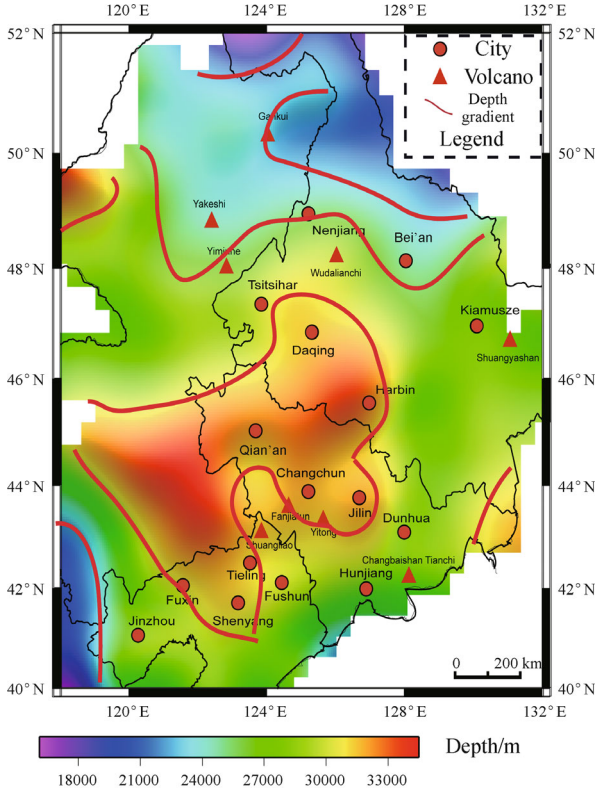

Fig. 8 Map of the estimation depth of the Curie isothermal surface in the Songliao Basin

Acknowledgements This work has been supported financially by the National Science and Technology Major Project (2011ZX05009-001). We thank the China Aero Geophysical Survey & Remote Sensing Center (AGRS) and the Daqing Oilfield for providing the gravity and magnetic data used in this study. The two anonymous reviewers are thanked for their help to improve this contribution.

References

Ai Y S, Zheng T Y, Xu W W, He Y M, Dong D (2003). A complex 660 km discontinuity beneath northeast China. Earth Planet Sci Lett, 212 (1–2): 63–71

Albora A M, Ucan O N (2001). Gravity anomaly separation using 2-D wavelet approach and average depth calculation. Dogus Univ J, 3: 1–12

Beltrão J F, Silva J B C, Costa J C (1991). Robust polynomial fitting method for regional gravity estimation. Geophysics, 56(1): 80–89

Bi S W (1997). Earth system science and sustainable development (II) the research on the dynamics model and plume tectonics features of the universal theory of the tectonics. Syst Eng Theory Pract, 7: 59–68

Cheng S Y (2006). Regional Tectonic Charaeters and Meso-Cenozoic Basin Evolution in Northeastern China. Dissertation for Ph.D degree. China University of geosciences, Beijing (in Chinese with English abstract)

Duncan R A, Richards M A (1991). Hot spots, mantle plumes, flood basalts, and true polar wander. Rev Geophys, 29(1): 31–50

Hu X Z, Xu M J, Xie X A, Wang L S, Zhang Q L, Liu S W, Xie G A, Feng C G (2006). A characteristic analysis of aeromagnetic anomalies and Curie point isotherms in Northeast China. Chin J Geophys, 49(6): 1533–1681 (in Chinese)

Huang H L, Zhao D P (2006). High-resolution mantle tomography of China and surrounding regions. J Geophys Res, B09305, doi: 10.1029/2005JB004066

Lee D T L, Yamamoto A (1994). Wavelet analysis: theory and applications. Hewlett Packard journal, 45: 44–44

Li J, Chen Q F, Vanacore E, Niu F (2008). Topography of the 660-km discontinuity beneath northeast China: Implications for a retrograde motion of the subducting Pacific slab, Geophys Res Lett, 35, L01302

Li J Y (2006). Permian geodynamic setting of Northeast China and adjacent regions: closure of the Paleo-Asian Ocean and subduction of the Paleo-Pacific Plate, J Asian Earth Sci, 26, 207–224

Li X Q, Yuan X H (2003). Receiver functions in northeast China-implications for slab penetration into the lower mantle in northwest Pacific subduction zone. Earth Planet Sci Lett, 216(4): 679–691

Li Y, Oldenburg D W (1998). Separation of regional and residual magnetic field data. Geophysics, 63(2): 431–439

Liu G D, HAO T Y, Liu Y K (1996). The significance of gravity and magnetic research for knowing sedimentary basin. Prog Geophys, 11: 1–15 (in Chinese)

Mallat S (1989). Multifrequency Channel decomposition and wavelet models IEEE ANS. On Acoustics, 37:209–211

Mallick K, Sharma K K (1999). A finite element method for computation of the regional gravity anomaly. Geophysics, 64(2): 461–469

Mickus K L, Aiken C L V, Kennedy W D (1991). Regional-residual gravity anomaly separation using the minimum-curvature technique. Geophysics, 56(2): 279–283

Ren J Y, Tamaki K, Li S T, Junxia Z (2002). Late Mesozoic and Cenozoic rifting and its dynamic setting in Eastern China and adjacent areas. Tectonophysics, 344(3–4): 175–205

Shen X Z, Zhou H L (2009). The low-velocity layer at the depth of 620 km beneath Northeast China. Chin Sci Bull, 54(17): 3067–3075

Sun B, Wang L S, Dong P, Wu Y J, Li C B, Hu B, Wang C (2012). Integrated analysis on gravity and magnetic fields of the Hailar Basin, NE China: implications for basement structure and deep tectonics. Pure Appl Geophys, 169(11): 2011–2029

Wang X W, Liu Y Y (1997). Pre-mesozoic tectonic evolution and its relation with development of late Mesozoic basin in northeast China. Geoscience, 11(4): 434–443

Wu F Y, Sun D Y, Li H M, Wang X L (2001). The nature of basement beneath the Songliao Basin in NE China: geochemical and isotopic constraints. 2nd Symposium on Chemical Geodynamics

Xiao W J, Windley B, Hao J, Zhai M G (2003). Accretion leading to collision and the Permian Solonker suture, Inner Mongolia, China: termination of the Central Asian Orogenic Belt. Tectonics, 2002TC001484

Xu W L, Ji W Q, Pei F P, Meng E, Yu Y, Yang D B, Zhang X (2009). Triassic volcanism in eastern Heilongjiang and Jilin provinces, NE China: chronology, geochemistry, and tectonic implications. Journal of Asian Earth Sciences, 34(2009): 392–402

Xu Y, Hao T Y, Li Z W, Duan Q L, Zhang L L (2009). Regional gravity anomaly separation using wavelet transform and spectrum analysis. Journal of Geophysics and Engineering, 6: 279–287

Yang B J, Mu S M, Jin X, Liu C (1996). Synthesized study on the geophysics of Manzhouli-Suifenhe geoscience transect, China. Chin J Geophys, 39: 772–782 (in Chinese)

Yang W C, Shi Z Q, Hou Z Z (2001). Discrete wavelet transform for multiple decomposition of gravity anomalies. Chinese journal of geophysics, 44(4): 529–537

Zhang F X, Zhang X Z, Zhang F Q, Meng L S, Xue J (2010). Study of gravity field in Northeastern China area: classification of main structure lines and tectonic units using the improved three-directional small subdomain filtering. Chin J Geophys, 53(6): 1475–1485 (in Chinese)

Zhang M, Suddaby P, Thompson R N, Thirlwall M F, Menzies M A (1995). Potassic volcanic-rocks in NE China-geochemical on mantle source and magma genesis. J Petrol, 36(5): 1275–1303

Zhao D P (2004). Global tomographic images of mantle plumes and subducting slabs: insight into deep Earth dynamics, Phys Earth Planet Inter, 146, 3–34

Zhao Y, Yang Z Y, Ma X H (1994). Geotectonic transition from paleosian system and paleotethyan system to paleopacific active continental margin in eastern Asia. Chinese Journal of Geology, 29 (2): 105–119 (in Chinese)

Zhu G Z, Shi Y L, Paul T (2010). Subduction of the Western Pacific Plate underneath Northeast China: implications of numerical studies. Phys Earth Planet Inter, 178(1–2): 92–99